Unsteady Flow and Pressure Pulsation Characteristics Analysis of Rotating Stall in Centrifugal Pumps under Off Design Conditions

Xiaoran Zhao[1], Zhengwei Wang [1]*, Yexiang Xiao[1], Yongyao Luo[1], Lei Cao[1]

ISROMAC 2016

International Symposium on Transport Phenomena and Dynamics of Rotating Machinery

Hawaii, Honolulu

April 10-15, 2016

Abstract

Unsteady flow phenomena like rotating stall frequently occur in centrifugal pumps under off design conditions. Rotating stall could lead to flow instabilities and pressure pulsation, which affect the normal operation of pumps. The mechanism of rotating stall has not been sufficiently understood in previous researches. This paper aims to simulate the unsteady flow characteristics in a centrifugal pump by CFD, analyze pressure pulsations caused by rotating stall and explore the propagation mechanism of rotating stall. In current study, 3D unsteady numerical simulations were performed to model the unsteady flow within the entire flow passage of a centrifugal pump under conditions of $0.4Q_{BEP}$ and $0.6Q_{BEP}$. Though flow characteristics research, the generation and propagation of rotating stall are discovered. Additionally, frequencies and amplitudes of pressure pulsations related to rotating stall are investigated by spectrum analysis.

Keywords

Rotating Stall —Centrifugal Pumps —Pressure Pulsation

[1] *State Key Laboratory of Hydroscience and Engineering and Department of Thermal Engineering, Tsinghua University, Beijing, China*

***Corresponding author**: wzw@tsinghua.edu.cn

INTRODUCTION

Centrifugal pumps are widely used in industry. To ensure efficient utilization, it is important to operate centrifugal pumps in stable conditions. Unsteady flow phenomena, including rotating stall, rotor-stator interaction (RSI) and reverse flows, exist in centrifugal pumps under off design conditions. All of above flow patterns could possibly lead to instabilities and pressure pulsations. During the past few years, rotor-stator interaction is regarded as the most important factor for strong pressure pulsations with blade passing frequency. Rotating stall is also a primary cause of low frequency pressure fluctuations in centrifugal pumps.

When flow rate decreases sharply, flow separation develops, resulting to the passage blockage. This blockage will cause adjacent passage stalled, like the stall cell is propagating circumferentially. This phenomenon is called rotating stall. Rotating stall was firstly discovered and extensively studied in compressor turbines [1,2]. Much attention has been paid to the study on flow structures of rotating stall in pumps by both numerical and experimental methods. Yoshida [3] observed rotating stall in the vaned diffuser of a centrifugal pump in experiment. Sinha [4] described rotating stall phenomenon at the exit part of a centrifugal pump with vanned diffusers and revealed the relationship between rotating stall and pressure pulsation by PIV measurements. Sano [5] used CFD technology to explore rotating stall and pressure variation in a vaned diffuser of a pump and proved that the clearance between impeller and diffuser had an effect on occurrence regions of rotating stall.

Recently, more researchers concentrate on rotating stall studies. Li [6] built an understanding on rotating stall in mixed flow pump and found that adverse pressure gradient in the flow passage increased with stall development and influenced stall in turn. Yuan [7] investigated broadband noise and resonance caused by rotating stall in a centrifugal pump under small flow rate condition though frequency analysis. Lucius [8] argued that rotating stall could excite structural vibrations in pumps through numerical simulations. Despite those studies, the mechanism of rotating stall has not been sufficiently understood in previous researches.

In centrifugal turbomachinery research, both flow pattern study and pressure pulsation analysis are necessary. Cao [9] described three-dimensional turbulent flow in the entire flow passage of a shrouded centrifugal pump to understand energy losses caused by different factors. Yang [10] investigated vibration and noise generation mechanism of a double suction centrifugal fan based on analysis of the pressure fluctuations. The present paper applies CFD technology to simulate flow characteristics in a centrifugal pump, analyzes pressure pulsations caused by rotating stall and explores propagation mechanism of rotating stall.

1. Calculation Model

1.1 Parameters of Centrifugal Pump

The studied model is a centrifugal pump with three impeller blades. Computational domains are showed in Figure 1, including volute, impeller and suction pipe. The main parameters of this pump are presented in Table 1.

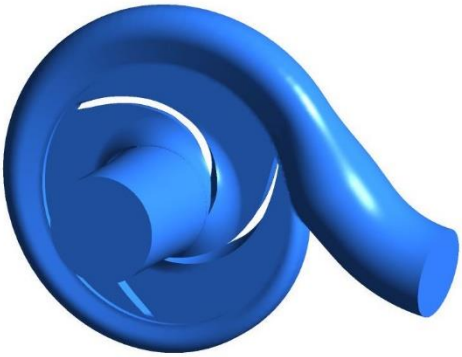

Figure 1 Computational pump

Table 1 Main parameters of computational pump

Parameters	Value
Nominal flow rate Q_N	200 m³/h
Designed head H_N	32 m
Rotating speed n	1450 r/min
Specific speed n_s ($n_s = \frac{3.65n\sqrt{Q_N}}{H_N^{3/4}}$)	92.7
Impeller outlet diameter d_2	350 mm
Impeller outlet width b_2	31 mm
Blade number Z	3

1.2 Turbulence Model and Boundary Conditions

In this research, ANSYS CFX is used to solve Reynolds-averaged Navier-Stokes (RANS) equations. RANS equations can analyze on both statistical average turbulence parameters and random fluctuating quantities. There are several turbulent models to describe turbulence program, including standard k-ε, RNG k-ε, standard k-ω, SST k-ω, and Reynolds stress model (RSM).

The incompressible continuity equation and the Reynolds time averaged Naviere-Stokes equations with the SST k-ω turbulence model was adopted in this paper.

1.3 Mesh Generation and Time Step Set

Mesh generation is a key step in the process of finite element modeling. Grid number, type and quality of the mesh affect the numerical simulation. Structure mesh cells generated by ANSYS ICEM were utilized in pump volute and suction pipe. Impeller structure mesh cells were produced by ANSYS Turbogrid. Cells near the solid wall were denser to capture the flow structure precisely, especially on blade surfaces.

To ensure both accuracy and efficiency of this simulation, mesh independent check was performed at optimum operating condition of 200 m³/h flow rate and 32 m head. The finally adopted mesh element amount in transient calculations was 3.35 million (0.7 million in suction pipe, 1.59 million in impeller and 1.06 million in volute). The structure mesh of impeller is showed in Figure 2.

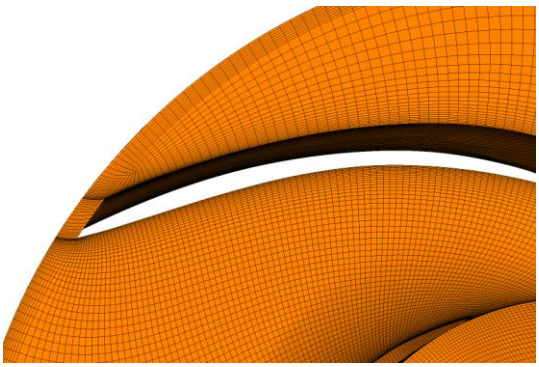

Figure 2. Structure mesh of impeller

The results of steady flow simulations were used as the initial flow flied of the unsteady simulations. The time step was set as 0.004138s, which is 1% of pump rotation period. Each pump revolution was calculated in a time sequence of 100 time steps.

2.4 Monitor Points Arrangement

Monitor points were set in each channel in the rotating impeller to record signals of pressure pulsation. Monitor points are set at pressure side, suction side and mid-passage of 0.5 span. Flow direction is from 11 to 16. Monitor points arrangement at one passage is presented in Figure 3.

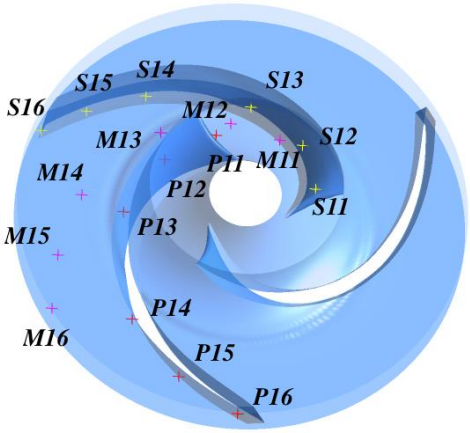

Figure 3. Monitor points arrangement

2. RESULTS AND DISCUSSION

In order to study flow patterns and pressure pulsation characteristics, unsteady simulations were performed for two different working conditions of $0.4Q_{BEP}$ and $0.6Q_{BEP}$.

2.1 Rotating Stall Flow Pattern Analysis

For the purpose of analyzing the impeller inner flow, numerous rotating periods were simulated. For $0.6Q_{BEP}$ working condition, Figure 4 describes the streamline in span-wise = 0.5 plane of impeller in the 14th rotating period. Smooth and blocked flow pattern alternatively presents in the impeller. Vortexes in one specific flow passage appear, expand, shrink and disappear repeatedly. Taking passage C for example, the flow pattern is relatively orderly at t = 0.5379s moment. There exists a flow separation at the inlet of pressure surface when impeller rotated by 36°, which develops into a serious vortex when impeller rotates from 36° to 180°. In

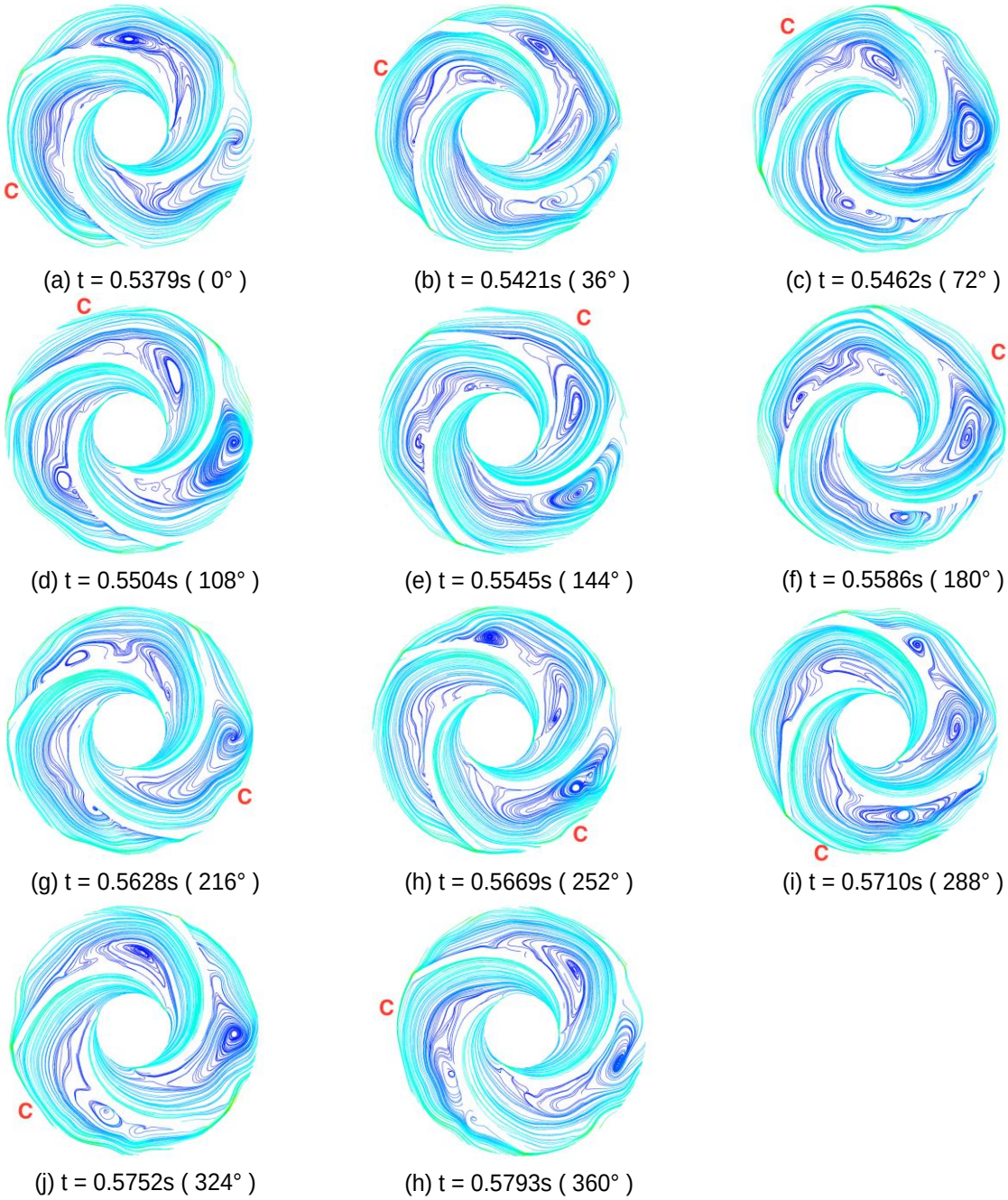

(a) t = 0.5379s (0°) (b) t = 0.5421s (36°) (c) t = 0.5462s (72°)

(d) t = 0.5504s (108°) (e) t = 0.5545s (144°) (f) t = 0.5586s (180°)

(g) t = 0.5628s (216°) (h) t = 0.5669s (252°) (i) t = 0.5710s (288°)

(j) t = 0.5752s (324°) (h) t = 0.5793s (360°)

Figure 4. Streamline in span-wise = 0.5 plane of 14th rotating period under 0.6QBEP working condition

the meanwhile, the vortex transports from inlet to outlet, decreases gradually, and finally tends to disappear when impeller rotates by 360°. The core of vortex locates at pressure surface during the whole rotating period. The changing trend of flow structures in other two passages is similar to passage C.

Besides vortexes appear and disappear sequentially in one passage, it is also found that stall cells propagate between flow passages. Figure 5 shows the transportation of stall cells in the impeller during the 14th rotating period under $0.6Q_{BEP}$ working condition. At t = 0.5379s moment, there exists an obvious vortex in passage A, which rotated by the opposite direct as the impeller. This stall cell obstructed flow and increased angle of attack in passage C, which cause stalls occurrence in passage C with the impeller rotation, as shown in Figure 5(b), (c). On the contrary, flow pattern in passage A tends to be smooth at the same time. In summary, the flow interaction leads to propagation of stall cells in the impeller by the reverse direction of impeller rotation.

λ_2-criterion is used to present the vortex structures to identify internal flow of the impeller. λ_2-criterion [11] was proposed by Jeong and Hussain in 1995. When ignoring the effect of disturbance and viscosity, the symmetrical parts in gradient of incompressible Navier-Stokes equations can be expressed as

$$\boldsymbol{S}^2 + \boldsymbol{\Omega}^2 = -\frac{1}{\rho}\nabla(\nabla p)$$

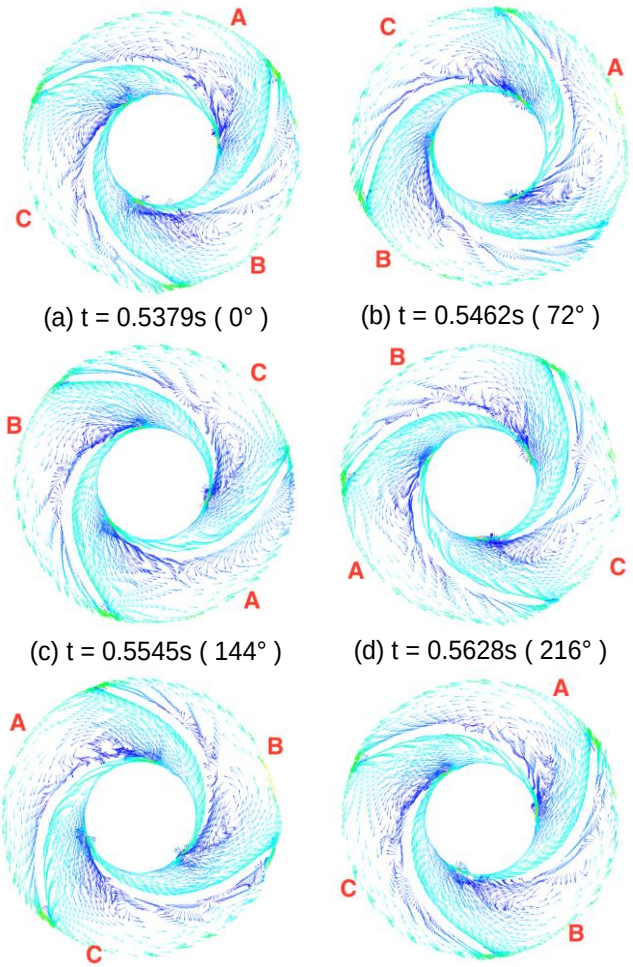

Figure 5. Vector in span-wise = 0.5 plane of 14th rotating period under 0.6Q_{BEP} working condition

(a) 0.4Q_{BEP} (b) 0.6Q_{BEP}

Figure 6. Flow vortex structures under 0.4QBEP and 0.6Q_{BEP} working conditions ($\lambda_2 = -300000m^{-2}$)

Assume that eigenvalues of the symmetric tensor is λ_1, λ_2 and λ_3, $\lambda_1 \geq \lambda_2 \geq \lambda_3$, $\lambda_2 < 0$. Figure 6 shows vortex structures in the impeller under 0.4Q_{BEP} and 0.6Q_{BEP} working conditions ($\lambda_2 = -300000m^{-2}$). When comparing the two working conditions, it is demonstrated that rotating stall is more fully developed under 0.4Q_{BEP} working conditions, which is farther from the optimum condition.

2.2 Unsteady Pressure Pulsation Characteristics Analysis

In order to investigate unsteady characteristics of rotating stall, pressure pulsation signals of 54 monitor points under both 0.4Q_{BEP} and 0.6Q_{BEP} working conditions are collected and analyzed. Figure 7 reveals change rules of pressure signals with time in 4 rotating periods, taking monitor points P14 and S14 for example. Time domain charts of pressure pulsation indicate that pressure changes periodically with time and has one wave crests and troughs in one rotating period, which are mainly caused by rotor-stator interaction.

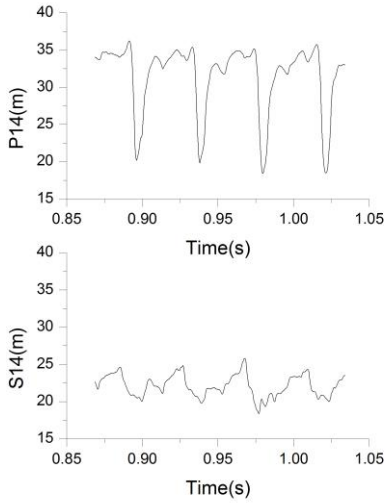

Figure 7. Change rules of pressure signals with time of monitor point np112 and np122

Figure 8 presents pressure spectra of monitor points in one passage C. As observed, dominant frequencies of pressure pulsation on blade points are rotating frequency (f = fn) and other harmonic frequencies (f = 2fn, 3fn, …). Besides these frequencies, it is found that a frequency (f = 0.6fn) appears at monitor points M14-M16, P14-P16, which is considered as the frequency of rotating stall. Many researches have shown that the spread speed of stall cells is less than rotating speed of the impeller, which means the characteristic frequency of rotating stall is lower than rotation frequency. Results mentioned above agree well with this conclusion. The spectra also imply that the pressure pulsation amplitudes of rotating stall are more obvious at monitor points P14-P16. This finding indicates that stall cells appear downstream at the pressure side, which accords with the flow pattern analysis in Figure 4.

Bisides the pressure pulsation of stall cells propagating, rotating stall could impact on pressure pulsations caused by RSI. Amplitudes of frequency (f = 3fn) at monitor points P15 and P16 are higher than that of frequency (f = 2fn), which could be explained as follows : when stall cells pass by the volute tongue, the flow interaction will lead to pressure pulsations. The acting mechanism and influence needs further study.

Figure 9 is pressure spectra of monitor point P15 under two working conditions. The unsteady pressure pulsation characteristics under 0.4Q_{BEP} working conditions is similar to 0.6Q_{BEP}. The frequency components are more complicated and the amplitudes of rotating frequency and its harmonic frequencies are higher under 0.4Q_{BEP} working conditions. It is demostrated that flow patterns are more complex when the flow rate is smaller apart from the optimal working condition.

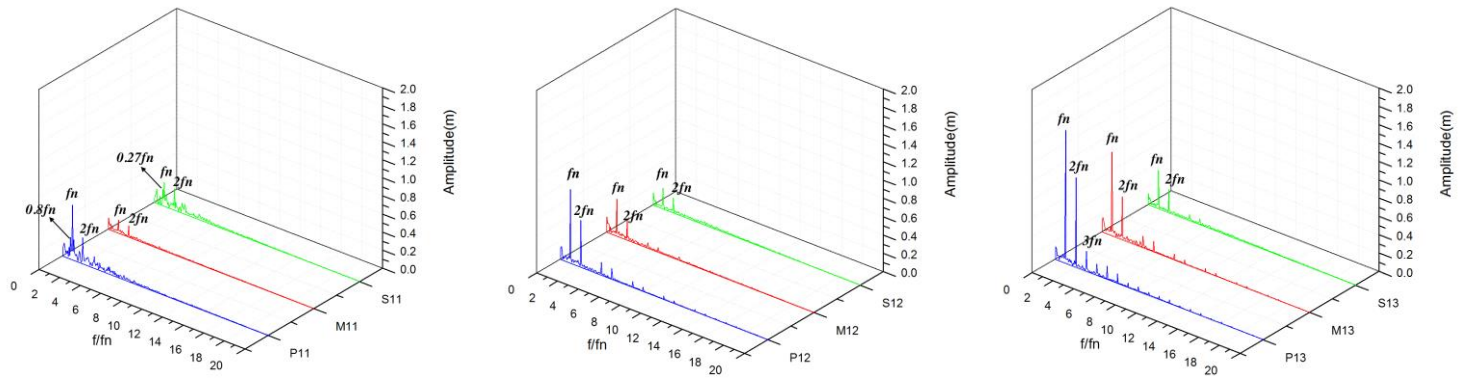

(a) P11, M11 and S11 (b) P12, M12 and S12 (c) P13, M13 and S13

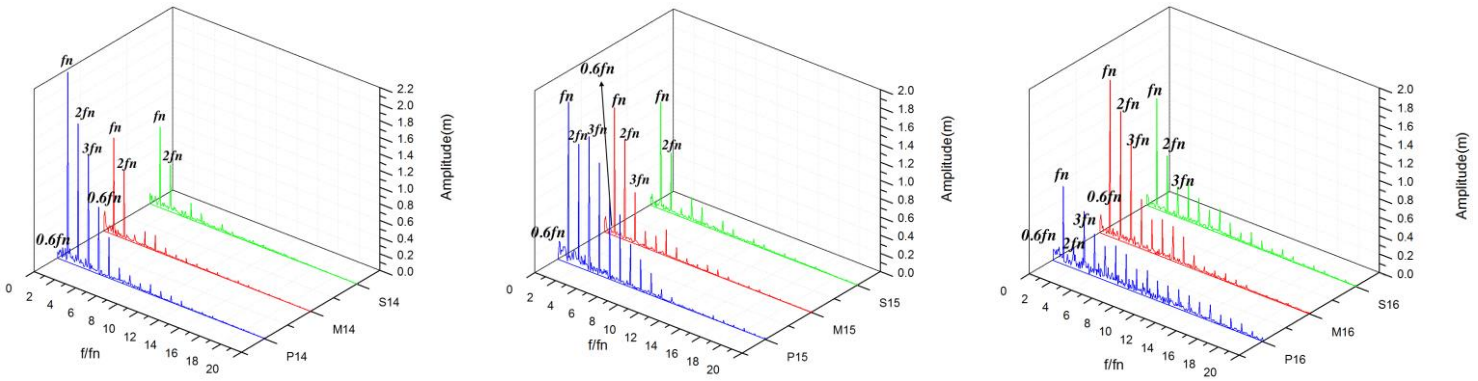

(d) P14, M14 and S14 (e) P15, M15 and S15 (f) P16, M16 and S16

Figure 8. Pressure spectra of 54 monitor points in the impeller under $0.6Q_{BEP}$ working condition

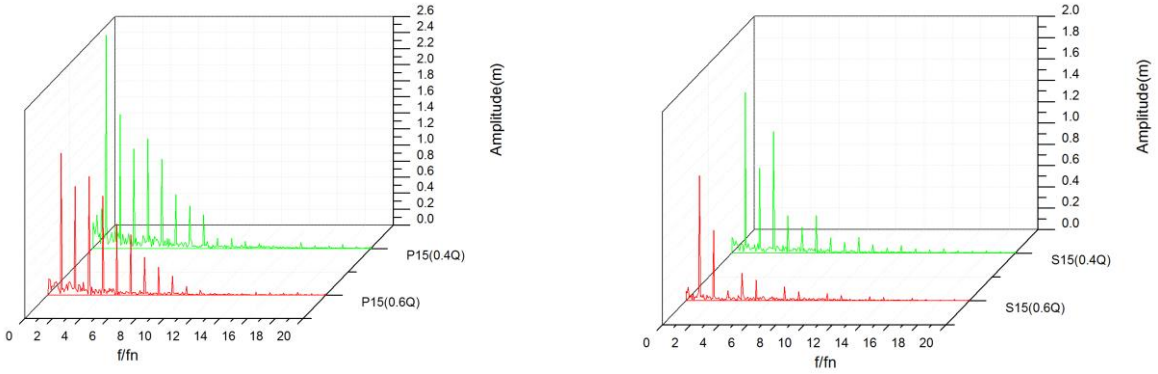

(a) P15 (b) S15

Figure 9. Pressure spectra of monitor points P15 and S15 under $0.4Q_{BEP}$ and $0.6Q_{BEP}$ working conditions

3. Conclusions

Numerical simulations of the internal unsteady flow in a centrifugal pump reasonably illustrate the flow characteristics inside the pump. When operating at part load condition (60% BEP and 40% BEP), there exists obvious rotating stall phenomenon in the pump impeller.

(1) In flow pattern analysis, it is found that stall cells appear, expand, shrink and disappear sequentially in one flow passage. Due to the blockage caused by rotating stall, flow separation occurs at the impeller inlet, which leads to stall cells propagation between passages. The vorticity research implies that rotating stall develops more seriously under lower flow rate working condition.

(2) Since the unsteady pressure pulsation inside the pump could cause variations, the pressure signals at various monitor points in the impeller were analyzed. The results indicate that rotating stall frequency is lower than rotating frequency and that the interaction between stall cells and volute tongue could have an influence on RSI pressure pulsation. There is evident pressure amplitudes from rotating stall downstream at the pressure side, which agrees well with the flow pattern analysis.

ACKNOWLEDGMENTS

Special thanks are due to the State Key Program of National Science of China (Grant No. 51439002), National Natural

Science Foundation of China (No. 51279083), Special Funds for Marine Renewable Energy Projects (Grant No. GHME2012GC02), State Key Laboratory of Hydroscience and Engineering (Grant No. 2014-KY-05) for supporting the present work.

REFERENCES

[1] Emmons, H.W., Pearson, C.F., and Grant, H.P. 1955, Compressor Surge and Stall Propagation [J], *Transactions of the ASME*, Vol. 79.

[2] Day I J. Stall inception in axial flow compressors [J]. *Journal of Turbomachinery*, 1993, 115(1):1-9.

[3] Yoshida, Y., Murakami, Y., Tsurusaki, H., and Tsujimoto, Y., 1991, Rotating Stalls in Centrifugal Impeller/Vaned Diffuser Systems [J], ASME, FED-Vol. 107, pp. 125–130.

[4] Sinha M, Pinarbasi A, Katz J. The Flow Structure During Onset and Developed States of Rotating Stall Within a Vaned Diffuser of a Centrifugal Pump [J]. *Journal of Fluids Engineering*, 2001, 123(3):490-499.

[5] Sano T, Yoshida Y, Nakamura Y, et al. Numerical Study of Rotating Stall in a Pump Vaned Diffuser [J]. *Journal of Fluids Engineering*, 2002, 124(2):363-370.

[6] Li X, Yuan S, Pan Z, et al. Dynamic Characteristics of Rotating Stall in Mixed Flow Pump [J]. *Journal of Applied Mathematics*, 2013, 2013(20):4819-4828.

[7] Yuan S, Yang J, Yuan J, et al. Experimental investigation on the flow-induced noise under variable conditions for centrifugal pumps [J]. *Chinese Journal of Mechanical Engineering*, 2012, 25(3):456-462.

[8] Lucius A, Brenner G. Numerical Simulation and Evaluation of Velocity Fluctuations During Rotating Stall of a Centrifugal Pump [J]. *Journal of Fluids Engineering*, 2011, 133(8):602-610.

[9] Cao Lei, Zhang Yiyang, Wang Zhengwei, Xiao Yexiang, Liu Changjun. Effect of axial clearance on the energy performance of an enclosed-impeller centrifugal pump with vice blades. *Journal of Fluids Engineering*. 2015; 137(7):071101-071101-10.

[10] Yang Jing, Meng Long, Zhou Lingjiu, Luo Yongyao, Wang Zhengwei. Unsteady internal flow field simulations in a double suction centrifugal fan, *Engineering Computations*. 2013, 30(3): 345-356.

[11] Chakraborty P, Balachandar S, Adrian R J. On the relationships between local vortex identification schemes[J]. *Journal of Fluid Mechanics*, 2005, 535: 189-214.